Hindawi
Advances in High Energy Physics
Volume 2019, Article ID 2526897, 11 pages
https://doi.org/10.1155/2019/2526897

Research Article

Nonperturbative Uncertainties on the Transverse Momentum Distribution of Electroweak Bosons and on the Determination of the W Boson Mass at the LHC

Giuseppe Bozzi [1,2] **and Andrea Signori** [3]

[1] *Dipartimento di Fisica, Università di Pavia, Via Bassi 6, I-27100 Pavia, Italy*
[2] *INFN, Sezione di Pavia, Via Bassi 6, I-27100 Pavia, Italy*
[3] *Physics Division, Argonne National Laboratory, 9700 S. Cass Avenue, Lemont, IL 60439, USA*

Correspondence should be addressed to Andrea Signori; asignori@anl.gov

Received 10 December 2018; Accepted 14 February 2019; Published 17 March 2019

Guest Editor: Daniel Pitonyak

In this contribution we present an overview of recent results concerning the impact of a possible flavour dependence of the intrinsic quark transverse momentum on electroweak observables. In particular, we focus on the q_T spectrum of electroweak gauge bosons produced in proton-proton collisions at the LHC and on the direct determination of the W boson mass. We show that these effects are comparable in size to other nonperturbative effects commonly included in phenomenological analyses and should thus be included in precise theoretical predictions for present and future hadron colliders.

1. Introduction

Electroweak precision observables are interesting benchmarks to test the limits of the Standard Model and to discriminate between different scenarios for new physics. The mass of the W boson, m_W, is an example of such an observable.

The Standard Model prediction for the W boson mass from the global fit of the electroweak parameters ($m_W = 80.356 \pm 0.008$ GeV) [1] has a very small uncertainty that represents a natural target for the precision of the experimental measurements of m_W at hadron colliders.

Direct measurements of m_W at hadronic colliders have been performed at the Tevatron $p\overline{p}$ collider with the D0 [2] and CDF [3] experiments and at the LHC pp collider with the ATLAS [4] experiment, with a total uncertainty of 23 MeV, 19 MeV, and 19 MeV, respectively. The current world average, based on these measurements and the ones performed at LEP, is $m_W = 80.379 \pm 0.012$ GeV [5]. Figure 1 presents an overview of these measurements compared to the electroweak global fit. The CPT theorem [6, 7] implies that the mass and lifetime of a particle and its antiparticle are the same. The ATLAS measurement of the W^+ and W^- mass difference yields $m_{W^+} - m_{W^-} = -29 \pm 28$ MeV [4]. The experimental determinations are based on a template-fit procedure applied to differential distributions of the W decay products: in particular, the transverse momentum of the final lepton, p_T^ℓ, the transverse momentum of the neutrino p_T^ν (only at the Tevatron), and the transverse mass m_T of the lepton pair (where $m_T = \sqrt{2p_T^\ell p_T^\nu \ (1 - \cos(\phi_\ell - \phi_\nu))}$, with $\phi_{\ell,\nu}$ being the azimuthal angles of the lepton and the neutrino, respectively). The transverse momentum of the lepton pair, though not directly used in the template-fit procedure, is relevant for reweighing purposes (see, for instance, Sec. 6 of Ref. [4]).

At leading order the W boson is produced with zero transverse momentum (q_T^W), but perturbative and nonperturbative corrections give rise to nonvanishing values of q_T^W. While perturbative and flavour-independent nonperturbative corrections have received much attention and reached a high level of accuracy (see, for instance, Ref. [8, 9] and references therein), a possible flavour dependence of the intrinsic

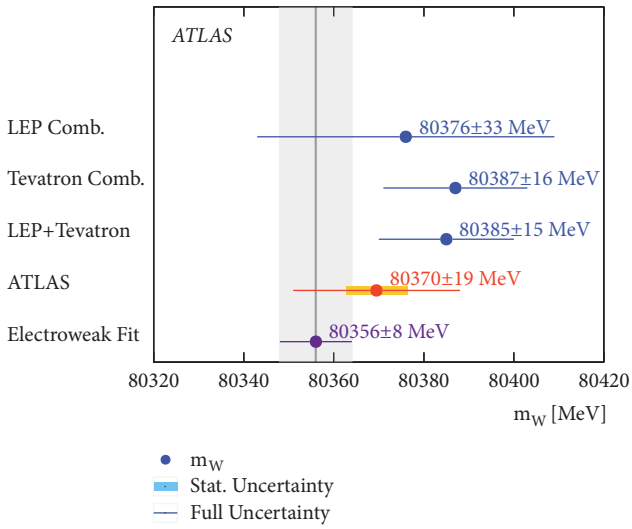

FIGURE 1: Overview of the measurements of the W boson mass. The indirect determination via the electroweak fit sets the precision for the measurements via direct determinations. Figure from Ref. [4].

transverse momentum (k_T) of the initial state partons has been less investigated.

In Figure 2, we examine the decomposition in flavour channels of the cross section for Z and $W^{\pm}$ production differential with respect to q_T^V, $V = Z, W^{\pm}$. A nontrivial interplay among the different flavours and the gluon is observed. The role of the gluon becomes increasingly important at larger values of the transverse momentum. In the region of the peak, instead, the dominant channels involve combinations of u_{val}, d_{val}, $\overline{u}$, and $\overline{d}$ (where $a = a_{val} + a_{sea}$ and $\overline{a} = a_{sea}$). For this reason, we consider it important to study the impact of flavour-dependent effects on the production of electroweak bosons and on the determination of m_W.

In this contribution we give an overview of selected studies related to flavour-dependent effects, focusing in particular on the results obtained in [10, 11], showing that they can be nonnegligible compared to other sources of theoretical uncertainty and should thus be included in precision physics programs at hadron colliders.

2. Formalism

In processes with a hard scale Q and a measured transverse momentum q_T, for instance, the mass and the transverse momentum of an electroweak boson produced in hadronic collisions, we can distinguish three regions: a small q_T region ($q_T \ll Q$), where large logarithms of q_T/Q have to be properly resummed; a large q_T region ($q_T \gtrsim Q$), where fixed-order perturbation theory provides reliable results; and an intermediate region, where a proper matching procedure between all-order resummed and fixed-order contributions is necessary. For a concise discussion (and for additional relevant references) on the development of the different frameworks available to resum the logs of q_T/Q and on their matching to fixed-order perturbative calculations, we refer the reader to [18–25].

In the Transverse-Momentum-Dependent (TMD) factorisation framework [26], the unpolarized TMD Parton Distribution Function (TMD PDF) for a parton with flavour a, carrying a fraction x of longitudinal momentum at a certain scale Q^2, can be written in b_T-space (where b_T is the variable Fourier-conjugated to the partonic transverse momentum k_T) as

$$\tilde{f}_1^a\left(x, b_T; Q^2\right) = \sum_{i=q,\overline{q},g} \left(C_{a/i} \otimes f_1^i\right)\left(x, b_T, \mu_b^2\right) \cdot e^{S\left(\mu_b^2, Q^2\right)} e^{g_K\left(b_T, \boldsymbol{\lambda}\right) \ln\left(Q^2/Q_0^2\right)} \tilde{f}_{\mathrm{NP}}^a\left(b_T, \boldsymbol{\lambda}'\right), \tag{1}$$

where μ_b is the b_T-dependent scale at which the collinear parton distribution functions are computed and Q_0 is a hadronic mass scale. Equation (1) is a generic schematic implementation of the perturbative and nonperturbative components of a renormalized TMD PDF. Depending on the chosen perturbative accuracy, S includes the UV-anomalous dimension of the TMD PDF and the Collins-Soper kernel. Also, in principle the TMD PDF depends on two kinds of renormalization scales, related to the renormalization of UV and light-cone divergences. Here we specify their initial and final values as μ_b and Q, respectively. Moreover, the perturbative scales can be chosen in position or momentum space [12, 14, 27–30]. For the implementation of all these details, we refer the reader to the description of the public codes that we are going to discuss.

The C coefficients in (1), also called Wilson coefficients for the TMD distribution, are calculable in perturbation theory and are presently known at order α_s^2 in the unpolarized case [21, 31, 32]. They are convoluted with the corresponding collinear parton distribution functions f_1^i according to

$$\left(C_{a/i} \otimes f_1^i\right)\left(x, b_T, \mu_b^2\right) = \int_x^1 \frac{du}{u} C_{a/i}\left(\frac{x}{u}, b_T, \alpha_s\left(\mu_b^2\right)\right) f_1^i\left(u; \mu_b^2\right), \tag{2}$$

The perturbative part of the evolution, the S factor in (1), can be written as

$$S\left(\mu_b^2, Q^2\right) = \int_{\mu_b^2}^{Q^2} \frac{d\mu^2}{\mu^2} \gamma_F\left[\alpha_s\left(\mu^2\right), \frac{Q^2}{\mu^2}\right] - K\left(b_T; \mu_b^2\right) \log \frac{Q^2}{\mu_b^2}. \tag{3}$$

It involves, in principle, the UV-anomalous dimension γ_F and the Collins-Soper kernel K, which can be decomposed as

$$\gamma_F\left[\alpha_s\left(\mu^2\right), \frac{Q^2}{\mu^2}\right] = -\left[\sum_{k=1}^{\infty} A_k \left(\frac{\alpha_s\left(\mu^2\right)}{4\pi}\right)^k\right] \ln\left(\frac{Q^2}{\mu^2}\right) + \sum_{k=1}^{\infty} B_k \left(\frac{\alpha_s\left(\mu^2\right)}{4\pi}\right)^k,$$

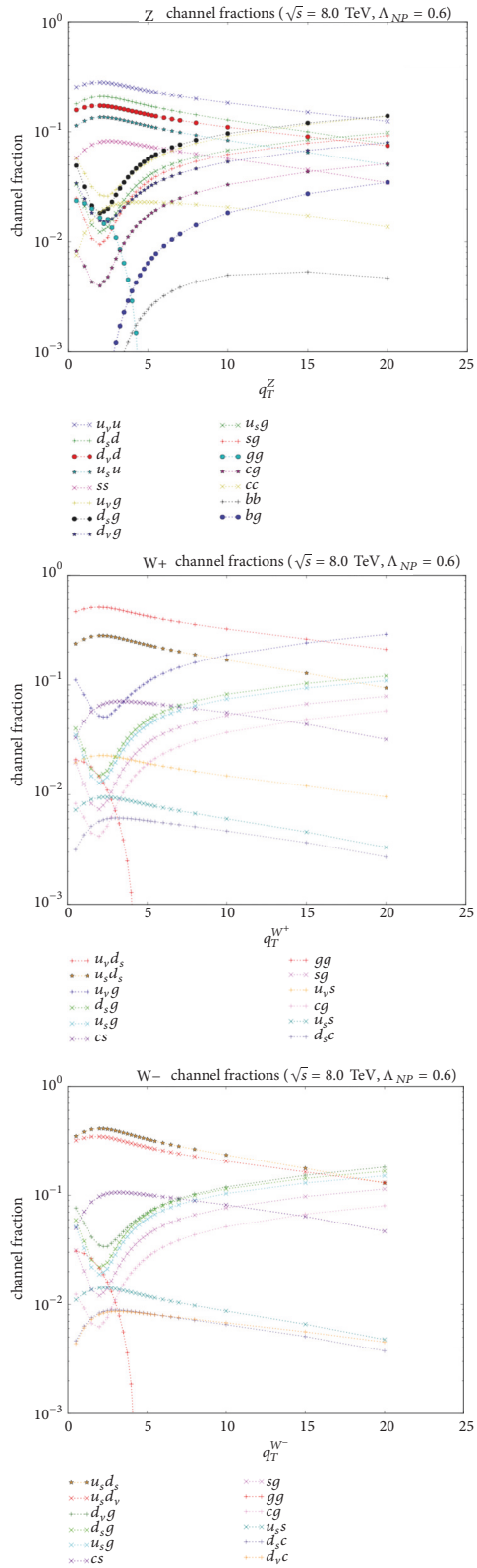

FIGURE 2: From top to bottom: the decomposition in flavour channels of the cross section $d\sigma/dq_T$ for Z, W^+, W^- production differential with respect to the transverse momentum of the produced electroweak boson q_T^V, $V = Z, W^+, W^-$. The rapidity and the collinear momentum fractions have been integrated over the kinematically allowed ranges. The cross section is calculated by means of `CuTe` [12] at LHC $\sqrt{s} = 8$ TeV. The nonperturbative correction is implemented as a flavour-independent Gaussian smearing, governed by the parameter Λ_{NP} (see [12] and the Appendix). The channels add to one.

$$K\left(b_T, \mu_b^2\right) = \sum_{k=1}^{\infty} d_k \left(\frac{\alpha_s\left(\mu^2\right)}{4\pi}\right)^k. \tag{4}$$

The A_k and B_k coefficients are known up to NNNLL (at least, their numerical value) and the integration of the Sudakov exponent in (4) can be done analytically up to NNNLL (for the complete expressions see, e.g., [33–35]). The perturbative coefficients of the kernel K are also known analytically up to NNNLL.

A well-known problem in the implementation of the QCD evolution of transverse-momentum-dependent distributions (TMDs) is the divergent behaviour at large b_T caused by the QCD Landau pole. Two common prescriptions to deal with this divergence consist in replacing b_T with a variable that saturates at a certain $b_{T\max}$, as suggested by the CSS formalism [26, 36], or perform the b_T integration on the complex plane in such a way that the Landau pole is never reached [37]. On the other hand, also the small b_T region needs to be regularized, in order to eliminate unjustified contributions from the evolution of TMDs in the intermediate and large q_T regions and to recover the expression for the cross section in collinear factorisation upon integration over q_T. Several prescriptions exist [14, 20, 33, 38, 39] also in this case. In `CuTe` the cross section is calculated integrating b_T on the real axis and the initial value for the renormalization scale is $\mu_b \equiv \mu_c \doteq q_T + q_\star$, where the scale $q_\star$ screens the cross section from receiving long-distance contributions. The definition of $q_\star$ is given analytically in (3.2) in [12] and its numerical value is $\sim$ 1.88 GeV. Also in `DyRes` the cross section is calculated integrating b_T on the real axis. The initial scale is defined as $\mu_b = 2e^{-\gamma_E}/b_\star$ [28] and a freezing prescription is given for $b_\star$ in order to avoid the Landau pole; see (2.18) in [28]. The value of the cutoff parameter $b_{T\max}$ in b_T space is a function of the renormalization scale μ_R and the resummation scale Q: $b_{max}\ Q \sim 1.2 \cdot 10^3\ \mu_R/m_Z$. In our case, $\mu_R = Q = m_W$. In `DyqT`, instead, the integration over b_T is performed using the complex-b prescription [37]; thus no freezing parameter is needed and μ_b is just defined as $2e^{-\gamma_E}/b_T$ [27].

Two intrinsically nonperturbative factors are introduced in (1) in order to account for the large b_T behavior. The first one is named $g_K(b_T; \boldsymbol{\lambda})$ in the TMD/CSS literature [26]. It embodies the nonperturbative part of the evolution, which is flavour-independent. The second one, $\widetilde{f}^a_{\mathrm{NP}}(b_T; \boldsymbol{\lambda}')$, accounts for a flavour-(in)dependent intrinsic transverse momentum of the parton with flavour a. We note that, in principle, this contribution can be also x-dependent (see, e.g., [15]), but in this treatment we choose to neglect this feature. The $\boldsymbol{\lambda}$ and $\boldsymbol{\lambda}'$ are (vectors of) nonperturbative parameters that can be fit to data. The $\boldsymbol{\lambda}'$ parameters are related to the quantity $\langle \boldsymbol{k}_T^2 \rangle_a$. For example, in case of a simple Gaussian functional form, $e^{-\lambda' b_T^2}$, we have $\lambda' = \langle \boldsymbol{k}_\star^2 \rangle_a / 4$. For both the nonperturbative factors g_K and $\widetilde{f}^a_{\mathrm{NP}}$, several implementations have been discussed; see, e.g., [14, 23] and references therein. In particular, a kinematic- and flavour-dependent Gaussian parametrisation has been proposed in [15, 29].

The studies that we discuss make use of three different computational tools: `CuTe` [12], `DyqT` [27], and `DYRes` [28]. `CuTe` is based on resummed expressions calculated using soft-collinear effective theory (SCET). It gives the transverse momentum spectrum of on-shell electroweak bosons up to NLO ($\mathcal{O}(\alpha_s)$) accuracy in the C Wilson coefficients and up to NNLL in the Sudakov exponent (`CuTe` is labelled NNLL in the SCET language but NNLL$'$ in standard pQCD language. The accuracy of NNLL$'$ is considered lower than that of the full NNLL, in which Wilson coefficients are computed at NNLO).

`DyqT` and `DYRes` are based on [27, 28] and perform soft gluon resummation in b_T-space. The first computes the q_T spectrum of an electroweak boson produced in hadronic collisions. The second also provides the full kinematics of the vector boson and of its decay products, allowing for the application of arbitrary cuts on the final-state kinematical variables and giving differential distributions in form of bin histograms. The accuracy of both codes is up to NNLL in the resummed part and up to NLO ($\mathcal{O}(\alpha_s^2)$) at large q_T.

A simple Gaussian parametrisation of the nonperturbative effects is present in these codes, as in most of the computational tools used to analyse the electroweak observables relevant for the determination of the W boson mass. A single nonperturbative parameter, g_{NP}, usually encodes both the (flavour-independent) effect of g_K and the distribution in the (potentially flavour-dependent) intrinsic transverse momentum (`ResBos` [40] is a counter-example, but it does not account for the flavour dependence of the intrinsic transverse momentum):

$$e^{-g_{NP} b_T^2} \equiv e^{2 g_K(b_T;\boldsymbol{\lambda}) \ln(Q^2/Q_0^2)}\, \widetilde{f}^a_{\mathrm{NP}}\left(b_T; \boldsymbol{\lambda}'\right) \widetilde{f}^{a'}_{\mathrm{NP}}\left(b_T; \boldsymbol{\lambda}'\right). \tag{5}$$

The values of the nonperturbative parameters used in fitting the W boson mass are usually obtained through fits on Z production data [40], for which the relevant partonic channels are of the type $q_i \overline{q}_i$, and then used to predict $W^\pm$ production, despite the process being sensitive to different partonic channels, $q_i \overline{q_j}$ ($i \neq j$). This procedure essentially neglects any possible flavour dependence of the intrinsic partonic transverse momentum.

In order to introduce the flavour dependence, one can simply decompose g_{NP} in the LHS of (5) into the sum $g^a_{NP} + g^{a'}_{NP}$, where the flavour indices span the range $a, a' = u_v, u_s, d_v, d_s, s, c, b, g$ (the subscripts referring to the valence and sea components, respectively), additionally disentangling the nonperturbative contribution to the evolution and the intrinsic transverse momentum distribution. Thus, for each parton with flavour a, the nonperturbative contributions $\widetilde{f}^a_{\mathrm{NP}}$ and g_K in (1) and (5) are included in the corresponding term in the flavour sum of the TMD factorisation formula. More details regarding the nonperturbative parameters in the codes under consideration have been collected in the Appendix.

3. Effects on the q_T Spectrum of the W

The impact of a flavour-dependent intrinsic $\langle \boldsymbol{k}_T^2 \rangle$ on the q_T spectrum of the electroweak bosons has been first studied in

Table 1: Summary of the shifts in GeV induced on the peak position in q_T spectra of $W^{\pm}/Z$, generated by different effects. "f.i." stands for flavour-independent, whereas "f.d." for flavour-dependent. "Max $W^{\pm}$" effect indicates the maximum shift induced on the peak position of the $W^{\pm}$ q_T spectrum by flavour-dependent variations of $\langle \boldsymbol{k}_T^2 \rangle$ that keep the peak of the Z q_T spectrum unchanged. For the values of the flavour-dependent non-perturbative parameters we refer the reader to [10].

	W^+		W^-		Z	
$\mu_R = \mu_c/2, 2\mu_c$	+0.30	−0.09	+0.29	−0.06	+0.23	−0.05
pdf (68% cl)	+0.03	+0.03	+0.04	+0.00	+0.03	−0.02
pdf (90% cl)	+0.03	−0.05	+0.06	−0.02	+0.05	−0.02
$\alpha_s = 0.118 \pm 0.003$	+0.14	−0.12	+0.14	−0.14	+0.15	−0.15
f.i. $\langle \boldsymbol{k}_T^2 \rangle = 1.0, 1.96$	+0.16	−0.16	+0.16	−0.14	+0.16	−0.15
f.d. $\langle \boldsymbol{k}_T^2 \rangle$ (max W^+ effect)	+0.09			−0.06	±0	
f.d. $\langle \boldsymbol{k}_T^2 \rangle$ (max W^- effect)		−0.03	+0.05		±0	

[10] and here we partly summarize the findings therein. Part of the analysis is devoted to the shifts induced in the position of the peak for the distribution in q_T^V, $V = W^+, W^-$ and Z. Flavour-independent (f.i.) and flavour-dependent (f.d.) variations of the average intrinsic transverse momentum squared are considered, together with the uncertainties associated to other nonperturbative factors, such as the collinear PDFs, the renormalisation scale, and the value of the strong coupling constant. As justified in Section 1 and Figure 2, it is assumed that the intrinsic transverse-momentum depends on five flavours only: u_v, d_v, u_s, d_s, s, where s collectively refers to the strange, charm, and bottom quarks and to the gluon.

The numerical results are obtained by means of a modified (i.e., flavour-dependent) version of `CuTe` [12]. Namely, the nonperturbative parameter $2\Lambda_{NP}^2$ (see the Appendix), which corrects the whole cross section at large b_T, is split into a sum of two flavour-dependent nonperturbative contributions, $\Lambda_{i,j}$, such that $\Lambda_i^2 + \Lambda_j^2 = 2\Lambda_{NP}^2$. This decomposition reabsorbs the nonperturbative contribution to QCD radiation into $\Lambda_{i,j}$. The flavour dependence of $\Lambda_{i,j}$ is compatible with the ratios fitted in [15]. The goal is to combine flavour dependent parameters in such a way to respect the values of Λ_{NP} fitted on the Z data, generating at the same time different values $\Lambda_{i,j}$ to be used in the calculation of the differential cross section for $W^{\pm}$ (we refer the reader to [10] for the precise values of $\Lambda_{i,j}$ used in the study).

The shifts (quantified in GeV) induced by different perturbative and nonperturbative contributions are summarized in Table 1. The renormalisation scale is varied between $1/2\mu_c$ and $2\mu_c$, with $\mu_c = q_T + q^*$, where q^* is the cutoff introduced in the Cute to avoid the Landau pole [12]. The scale in the hard part has not been varied. Regarding the impact of the collinear PDFs, the result shown in the table is the smallest interval which contains 68% or 90% of peak positions, computed for every member of the NNPDF3.0 set [41]. The strong coupling is varied by ±0.003 from the central value of 0.118.

The shift induced in the peak position from flavour-dependent $\langle \boldsymbol{k}_T^2 \rangle$ is smaller than that induced by scale variation, α_s variation, and flavour-independent $\langle \boldsymbol{k}_T^2 \rangle$, but comparable in magnitude. It is also bigger than the uncertainty from the PDF set, which is the only other uncertainty where the shifts are not almost perfectly correlated between the three vector bosons. With flavour-dependent variations of $\langle \boldsymbol{k}_T^2 \rangle$, the peaks of the W^+ and W^- distributions shift in different directions. Since the $\langle \boldsymbol{k}_T^2 \rangle$ parameters are selected under the constraint that the Z q_T-distribution is left unchanged (see Table 1), the channels for W^+ and W^- move in different directions. The anticorrelation of the shifts between W^+ and W^- is a peculiarity of the uncertainty generated by flavour-dependent variations of the intrinsic k_T. This means that the uncertainty stemming from the nonperturbative hadron structure in the transverse plane can affect the determination of m_{W^+} and m_{W^-} in different ways. Indeed, this feature nicely emerges in the analysis summarized in Section 4.

The analysis in [10] thus shows that the uncertainty on the peak position for $W^{\pm}$ bosons arising from the flavour dependence of the intrinsic transverse momentum is not negligible with respect to the other sources of theoretical uncertainties and comparable in magnitude with the uncertainties due to the collinear PDFs.

We now analyse the ratios of the q_T-differential cross section calculated with a flavour-independent set of nonperturbative parameters in $\widetilde{f}_{\mathrm{NP}}^a(b_T; \boldsymbol{\lambda}')$ over the same cross section calculated with flavour-dependent parameters. The results are presented in Figure 3 for Z, W^+, W^-. The calculation has been performed by means of a flavour-dependent modification of `DyqT`, where the nonperturbative contributions in (1) have been coded as

$$\exp\{-g_{NP}^a\} = \exp\left\{-\left[g_{evo}\ln\left(\frac{Q^2}{Q_0^2}\right) + g_a\right] b_T^2\right\}. \quad (6)$$

The values for g_{evo}, Q_0, g_a are taken from [14] and the flavour-dependence in g_a is inspired to the flavour ratios in [15]. The curves in Figure 3 correspond to 50 sets of flavour-dependent nonperturbative parameters built according to these criteria. The chosen perturbative accuracy is NLL [11, 13] and the collinear PDF set used is NNPDF3.1 [42].

As predicted by the TMD formalism, the effect induced by the non-perturbative corrections is more evident at low q_T. In particular, it is stronger for $q_T < 5$ GeV but sizable up to $q_T = 10$ GeV. The flavour dependence of the intrinsic transverse momentum can modify the shape of $d\sigma/dq_T$ by $\sim 5 - 10\%$ at very low transverse momentum. This observable affects the cross section differential with respect to the kinematics of the final state particles, namely, the distributions in p_T^{ℓ}, p_T^{γ}, m_T,

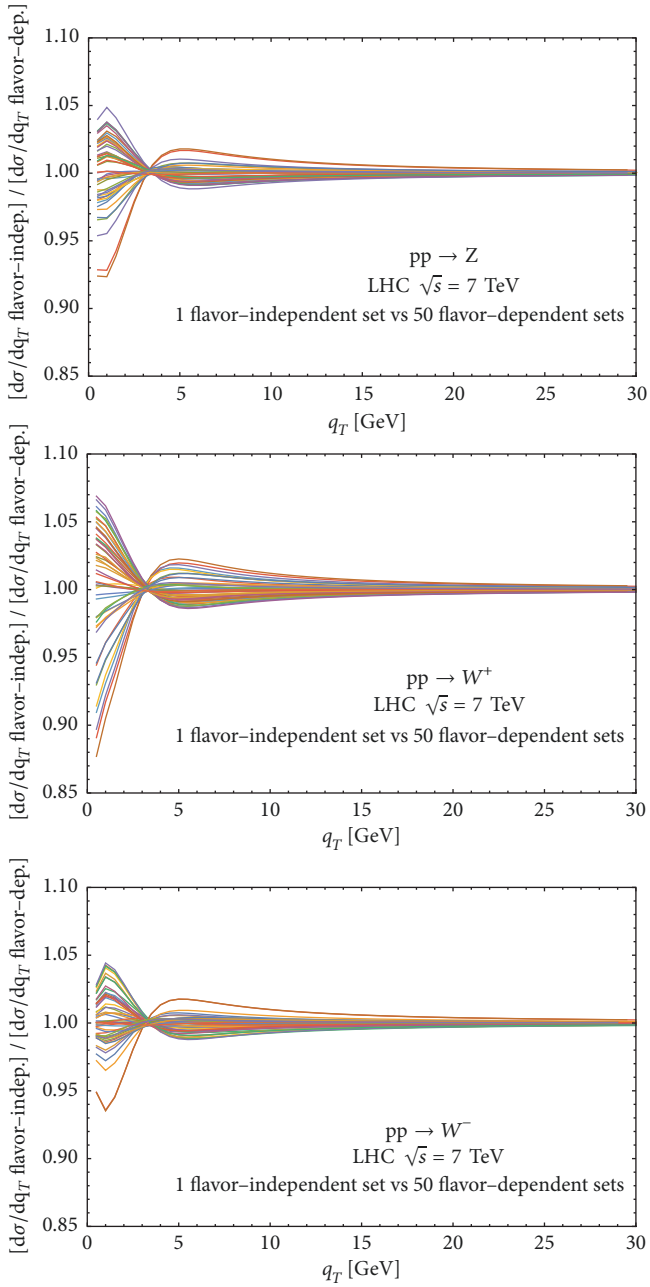

FIGURE 3: In these figures the ratio $(d\sigma^V/dq_T)(f.i.)/(d\sigma^V/dq_T)(f.d.)$ is plotted for the three different electroweak bosons ($V = Z, W^+, W^-$, respectively), with a single set of flavour-independent (f.i.) nonperturbative parameters in the transverse part of the TMD PDFs and 50 different flavour-dependent (f.d.) sets of the same parameters. The analysis has been performed at NLL [11, 13]. The values of the nonperturbative parameters have been chosen from the results in [14, 15].

and thus has an impact also on the determination of the W boson mass.

4. Impact on the Determination of the W Boson Mass

As previously mentioned, the measurements of m_W at hadron colliders rely on a template-fit procedure performed on selected observables, i.e., the distributions in the transverse mass of the lepton pair and the lepton/neutrino transverse momentum. Both CDF and D0 experiments at Tevatron use data from all the three observables. In the ATLAS case, however, the transverse momentum of the (anti)neutrino is used for consistency checks only, since it is affected by larger uncertainties with respect to m_T and p_T^ℓ.

In this section we consider selected results concerning the estimate of the uncertainties of nonperturbative origin on the determination of m_W. In particular, we focus on shifts of the $W^\pm$ mass induced by possible configurations for the flavour dependence of the intrinsic transverse momentum, and we

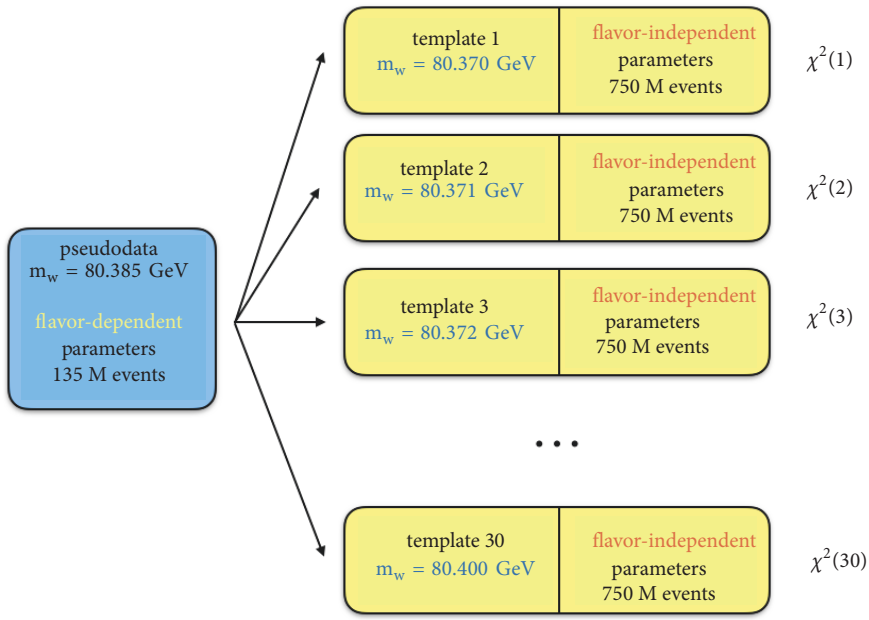

FIGURE 4: Flowchart for a template-fit procedure to estimate shifts in m_W induced by the flavour dependence of the intrinsic quark transverse momentum.

will compare them with the corresponding shifts generated by the uncertainties in the collinear PDFs.

In the template-fit procedure, several histograms are generated with a specific theoretical accuracy and description of detector effects, letting the fit parameter(s) (only m_W, in this case) vary in a range: the histogram best describing the experimental data selects the measured value for m_W. The details of the theoretical calculations used to compute the templates (the choice of the scales, of the collinear PDFs, of the perturbative order, the resummation of logarithmically enhanced contributions, the nonperturbative effects, etc.) affect the result of the fit and define the theoretical systematics.

This procedure can also be used to estimate the effect of each *single* theoretical uncertainty, by generating sets of pseudodata (with the same event generator used for the templates, but at a lower statistics) differing by the value of the parameter(s) controlling that uncertainty [43, 44]. Figure 4 contains a graphical illustration of the flowchart for the template-fit procedure, specified to the comparison of one set of pseudodata generated with flavour-dependent parameters with 30 templates generated with one set of flavour-independent parameters and 30 values of m_W (80385 ± 15 MeV with steps of 1 MeV). This method has been also used to estimate the shift in m_W induced by the variation of the collinear PDF set in fitting the transverse mass [16, 45] and the lepton p_T [17, 45] both at Tevatron and at the LHC in the central rapidity region of the produced electroweak boson ($|\eta| < 1.0$ for Tevatron and $|\eta| < 2.5$ for the LHC). A similar study dedicated to LHCb and its forward acceptance $2 < \eta < 4.5$ has been performed in [46].

In the transverse mass case, the total error (envelope) induced by three different PDF sets (CTEQ6.6 [47], MSTW2008 [48], and NNPDF2.1 [49]) is less than 10 MeV both at the Tevatron and at the LHC [16]. The results are shown in the left plot of Figure 5. The analysis has been performed at fixed-order NLO QCD ($\mathcal{O}(\alpha_s)$), thus without all-order resummation, since the m_T-shape is mildly sensitive to soft gluon emission from the initial state. The key factor in reducing the PDF uncertainty is the use of normalised differential distributions in the fitting procedure, in such a way to eliminate normalisation effects which are irrelevant for m_W.

A similar analysis applied to the lepton p_T observable reveals a much larger error due to PDF variations (CT10 [50], MSTW2008CPdeut [48], MMHT2014 [51], NNPDF2.3 [52], and NNPDF3.0 [41]), as shown in the right plot of Figure 5. While the individual sets provide nonpessimistic estimates ($\mathcal{O}(10\,\text{MeV})$), the distance between the best predictions of the various sets ranges between 8 and 15 MeV, and the total envelope ranges between 16 and 32 MeV (depending on the collider, the energy, and the final state) [16]. While soft gluon emission already provides a nonvanishing transverse momentum, additional contributions may come from the intrinsic transverse momentum of the colliding partons. The study of the impact of a possible flavour-dependent intrinsic k_T on the determination of m_W has been first performed in [11], using the same template-fit procedure described above and sketched in Figure 4, performed with modified versions of the `DYqT` [27] and `DYRes` [28] codes. In this case, the pseudodata are built with the Gaussian widths g_a associated with the different flavours in (6).

In order to estimate the impact of the flavour dependence, it is necessary to first identify those sets of flavor-dependent parameters which perform equally well in describing the Z boson q_T-spectrum, despite having potentially a very different flavor structure. This is motivated physically by the fact that the Z boson is produced from a $q_i\overline{q}_i$ pair whereas

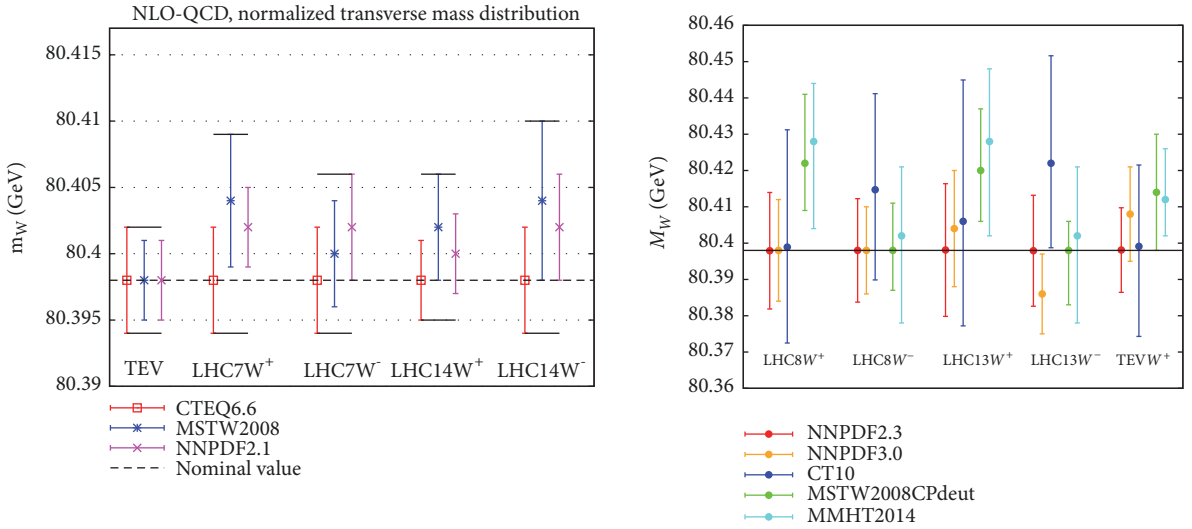

FIGURE 5: Shifts induced on m_W by the choice of different PDF sets, obtained through a template-fit performed on the transverse mass m_T (left) and the lepton p_T (right) observables (left figure from [16], right figure from [17]).

the $W^{\pm}$ bosons are produced from $q_i\overline{q}_j$ pairs, with $i \neq j$. For this reason, the Z is less sensitive to the flavor structure with respect to the $W^{\pm}$, and there might be flavor combinations that perform equally well in describing the q_T-spectrum of the Z but produce very different results when applied to the case of $W^{\pm}$. We identify as "Z-equivalent" those sets of flavor-dependent parameters in agreement with the Z transverse momentum distribution measured at hadron colliders [11]. To this extent

(i) a single flavour-independent (*i.e.*, using a version of Eq. (6) without a-dependence) q_T-spectrum for the Z boson is produced based on the parameters presented in Ref. [14];

(ii) each bin of this flavour-independent spectrum is assigned an uncertainty equal to the one quoted by the CDF and ATLAS experiments, which includes statistical and systematic components, neglecting the correlations;

(iii) several flavour-dependent sets for g_a in Eq. (6) are generated randomly within a variation range consistent with the information obtained in previous TMD fits (in particular, taking into account the estimate for the flavour-independent contribution to the non-perturbative part of the evolution obtained in Ref. [14]);

(iv) a flavour-dependent set is defined "Z-equivalent" if the associated q_T spectrum for the Z has a $\Delta\chi^2 \leq 1$ with respect to one generated by the flavour-independent set.

We note that the Z boson data alone are not able to discriminate between flavor-independent and flavor-dependent sets of nonperturbative parameters. Data from flavor-sensitive processes are needed, in particular from SIDIS.

The flavour-dependent sets for CDF and ATLAS who pass this filter are treated as the pseudodata of the template-fit procedure, while the flavour-independent one is used for the generation of the templates at high statistics. The number of events corresponds to 135M for the pseudodata and 750M for the templates. Only 9 sets out of the 30 ones which are "Z-equivalent" both with respect to CDF and ATLAS uncertainties have been investigated. The values of the flavour-dependent parameters for each set are given in Table 2. A summary of the shifts obtained through this procedure is given in Table 3.

TABLE 2: Values of the g^a_{NP} parameter in (6) for the flavours $a = u_v, d_v, u_s, d_s, s = c = b = g$. Units are GeV^2.

Set	u_v	d_v	u_s	d_s	s
1	0.34	0.26	0.46	0.59	0.32
2	0.34	0.46	0.56	0.32	0.51
3	0.55	0.34	0.33	0.55	0.30
4	0.53	0.49	0.37	0.22	0.52
5	0.42	0.38	0.29	0.57	0.27
6	0.40	0.52	0.46	0.54	0.21
7	0.22	0.21	0.40	0.46	0.49
8	0.53	0.31	0.59	0.54	0.33
9	0.46	0.46	0.58	0.40	0.28

The statistical uncertainty of the template-fit procedure has been estimated by considering statistically equivalent those templates for which $\Delta\chi^2 = \chi^2 - \chi^2_{min} \leq 1$. Overall, the quoted statistical uncertainty on the results in Table 3 is ±2.5 MeV.

Being the transverse mass mildly sensitive to the modeling of the $W^{\pm}$ transverse momentum, the corresponding shifts are compatible with zero considering the statistical uncertainty of the template-fit procedure. On the contrary, in the p_T^{ℓ} case the shifts can be incompatible with statistical fluctuations and are comparable to the ones induced by collinear PDFs, with an envelope of 15 MeV in the case of W^+ production and 11 MeV for W^- production. We also notice a

Table 3: Shifts in $m_{W^\pm}$ (in MeV) induced by the corresponding sets of flavour-dependent intrinsic transverse momenta outlined in Table 2 (statistical uncertainty: 2.5 MeV).

	Δm_{W^+}		Δm_{W^-}	
Set	m_T	p_T^ℓ	m_T	p_T^ℓ
1	0	-1	-2	3
2	0	-6	-2	0
3	-1	9	-2	-4
4	0	0	-2	-4
5	0	4	-1	-3
6	1	0	-1	4
7	2	-1	-1	0
8	0	2	1	7
9	0	4	-1	0

hint of a possible anti-correlation between the shifts in the W^+ and W^- cases, as it was also noticed in Section 3.

Along this line, we also stress that ATLAS measured $m_{W^+} - m_{W^-} = -29 \pm 28$ MeV [4]. From Table 3, we can infer that part of the discrepancy between the mass of the W^+ and the W^- can be artificially induced by not considering the flavour structure in transverse momentum. For example, the sets 1 and 2 in Table 2 feature $\delta m_{W^-} > \delta m_{W^+}$ (induced by p_T^ℓ). This implies that for templates built with sets 1 and 2, instead of flavour-independent values, the difference between the two masses would be reduced. An opposite result would be obtained if building templates with flavour-dependent sets for which $\delta m_{W^-} < \delta m_{W^+}$ (e.g., sets 3 and 5, for the p_T^ℓ case).

5. Outlook and Future Developments

The selected results presented in this contribution point out that the impact of a possible flavour dependence of the intrinsic partonic transverse momentum should not be neglected, even in the kinematic region where nonperturbative effects are expected to be small [53–55], such as for electroweak boson production at the LHC.

This kind of uncertainty directly affects the electroweak observables relevant for the measurement of m_W: the transverse momentum distribution for the W and the decay lepton and the transverse mass distribution of the lepton pair. The numerical results presented in Sections 3 and 4 indicate that flavour-dependent effects are comparable in size to other uncertainties of (non-)perturbative origin (for example, the choice of collinear PDF set). Thus, a flavour-blind analysis is not a sufficiently accurate option for a program of precision electroweak measurements at the LHC and at future colliders.

Moreover, in hadron colliders at a lower energy such as RHIC and a possible fixed-target experiment at the LHC, the non-perturbative effects can play an even more significant role (due to the larger x-values probed) and affect the study of polarised TMDs [56] and the structure of the light sea quarks [57].

A detailed knowledge of TMD distributions is thus important, not only for nucleon tomography beyond the collinear picture [58–66], but also to constrain fundamental parameters of the Standard Model, thus providing a direct connection between hadron physics and the high-energy phenomenology.

In light of these results, we call for improved investigations of the impact of nonperturbative effects linked to the hadron structure at hadron colliders and for the inclusion of these effects in the event generators employed in experimental and theoretical investigations of high-energy physics.

Appendix

Conventions for Nonperturbative Parameters

For convenience, we collect in this Appendix the naive translation of the nonperturbative parameters used in the numerical codes cited in the text. In the conventions of [15, 29], the nonperturbative parameters appear as

$$\mathrm{d}\sigma \propto \exp\left(-\frac{1}{4}\left(\left\langle k_T^2\right\rangle_{q_1} + \left\langle k_T^2\right\rangle_{q_2}\right) b_T^2\right). \tag{A.1}$$

In CuTe [12] there is a single nonperturbative parameter entering the cross section:

$$\mathrm{d}\sigma \propto \exp\left(-2\Lambda_{NP}^2 b_T^2\right). \tag{A.2}$$

The same happens in DyqT [27] and DYRes [28], in terms of the nonperturbative parameter g_{NP}:

$$\mathrm{d}\sigma \propto \exp\left(-g_{NP} b_T^2\right). \tag{A.3}$$

We obtain the parameter employed in CuTe as

$$\begin{aligned} \Lambda_{NP} &= \sqrt{\frac{1}{8}\left(\left\langle k_T^2\right\rangle_{q_1} + \left\langle k_T^2\right\rangle_{q_2}\right)}, \\ \Lambda_{NP} &= \sqrt{\frac{g_{NP}}{2}}. \end{aligned} \tag{A.4}$$

and similarly for the DYqT parameter:

$$\begin{aligned} g_{NP} &= \frac{1}{4}\left(\left\langle k_T^2\right\rangle_{q_1} + \left\langle k_T^2\right\rangle_{q_2}\right), \\ g_{NP} &= 2\Lambda_{NP}^2. \end{aligned} \tag{A.5}$$

The default value for Λ_{NP} discussed in [12] is $0.60\,\mathrm{GeV}^2$, whereas the conservative value for g_{NP} discussed in [27] is $0.8\,\mathrm{GeV}^2$ and in [28] is $1.2\,\mathrm{GeV}^2$.

Data Availability

The data used to support the findings presented in this study (authors: G. Bozzi, A. Signori) have been produced by means of the following public codes: (1) CuTe: https://cute.hepforge.org/ (2) DyqT: http://pcteserver.mi.infn.it/~ferrera/dyqt.html (3) DyRes: http://pcteserver.mi.infn.it/~ferrera/dyres.html. The data are available from the corresponding author upon request.

Conflicts of Interest

The authors declare that they have no conflicts of interest.

Acknowledgments

We thank Alessandro Bacchetta and Marco Radici for the fruitful collaboration on this topic, Alessandro Vicini for many suggestions and discussions, Chao Shi for carefully reading the manuscript, and Piet Mulders and Mathias Ritzmann for contributing to the investigations summarized in this article. Andrea Signori acknowledges support from the U.S. Department of Energy, Office of Science, Office of Nuclear Physics, Contract no. DE-AC02-06CH11357. Giuseppe Bozzi acknowledges support from the European Research Council (ERC) under the European Union's Horizon 2020 research and innovation program (Grant Agreement no. 647981, 3DSPIN).

References

[1] Gfitter Group collaboration, M. Baak, J. Cth et al., "The global electroweak fit at NNLO and prospects for the LHC and ILC," *The European Physical Journal C*, vol. 74, article 3046, 2014.

[2] V. M. Abazov, B. K. Abbott, B. S. Acharya et al., "Measurement of the W boson mass with the D0 detector," *Physical Review D*, vol. 89, article 012005, 2014.

[3] D. Ayres, H. Akimoto, A. Akopian et al., "Precise measurement of the W -boson mass with the collider detector at fermilab," *Physical Review D*, vol. 89, article 072003, 2014.

[4] M. Aaboud, G. Aad, B. Abbott et al., "Measurement of the W-boson mass in pp collisions at $\sqrt{s}$=7 TeV with the ATLAS detector," *The European Physical Journal C*, vol. 78, article 110, 2018.

[5] M. Tanabashi, K. Hagiwara, and K. Hikasa, "Review of Particle Physics," *Physical Review D*, vol. 98, article 030001, 1973.

[6] S. Weinberg, "The quantum theory of fields," in *Foundations*, vol. 1, Cambridge University Press, 2005.

[7] M. E. Peskin and D. V. Schroeder, *An Introduction to Quantum Field Theory*, Addison-Wesley, Massachusetts, Mass, USA, 1995.

[8] S. Alioli, A. B. Arbuzov, D. Y. Bardin et al., "Precision studies of observables in $pp \longrightarrow W \longrightarrow l\nu_l$ and $pp \longrightarrow \gamma, Z \longrightarrow l^+l^-$ processes at the LHC," *The European Physical Journal C*, vol. 77, article 280, 2017.

[9] C. M. Carloni Calame, M. Chiesa, H. Martinez et al., "Precision measurement of the W-boson mass: theoretical contributions and uncertainties," *Physical Review D*, vol. 96, article, 2017.

[10] A. Signori, *Flavor and evolution effects in TMD phenomenology [Ph.D. thesis]*, Vrije U, Amsterdam, Netherlands, 2016, https://userweb.jlab.org/~asignori/research/PhD_thesis_Andrea.pdf.

[11] A. Bacchetta, G. Bozzi, M. Radici, M. Ritzmann, and A. Signori, "Effect of flavor-dependent partonic transverse momentum on the determination of the W boson mass in hadronic collisions," *Physics Letters B*, vol. 788, pp. 542–545, 2019.

[12] T. Becher, M. Neubert, and D. Wilhelm, "Electroweak gauge-boson production at small q T: Infrared safety from the collinear anomaly," *Journal of High Energy Physics*, vol. 2012, no. 2, 2012.

[13] The ATLAS Collaboration, "Studies of theoretical uncertainties on the measurement of the mass of the W boson at the LHC," Tech. Rep. ATL-PHYS-PUB-2014-015, CERN, Geneva, Switzerland, 2014.

[14] A. Bacchetta, F. Delcarro, C. Pisano, M. Radici, and A. Signori, "Extraction of partonic transverse momentum distributions from semi-inclusive deep-inelastic scattering, Drell-Yan and Z-boson production," *Journal of High Energy Physics*, vol. 6, article 81, 2017.

[15] A. Signori, A. Bacchetta, M. Radici, and G. Schnell, "Investigations into the flavor dependence of partonic transverse momentum," *Journal of High Energy Physics*, vol. 11, article 194, 2013.

[16] G. Bozzi, J. Rojo, and A. Vicini, "The Impact of PDF uncertainties on the measurement of the W boson mass at the Tevatron and the LHC," *Physical Review D*, vol. 83, article 113008, 2011.

[17] G. Bozzi, L. Citelli, and A. Vicini, "Parton density function uncertainties on the W boson mass measurement from the lepton transverse momentum distribution," *Physical Review D*, vol. 91, article 113005, 2015.

[18] S. Catani, L. Cieri, D. de Florian, G. Ferrera, and M. Grazzini, "Universality of transverse-momentum resummation and hard factors at the NNLO," *Nuclear Physics. B. Theoretical, Phenomenological, and Experimental High Energy Physics. Quantum Field Theory and Statistical Systems*, vol. 881, pp. 414–443, 2014.

[19] M. Boglione, J. O. G. Hernandez, S. Melis, and A. Prokudin, "A study on the interplay between perturbative QCD and CSS/TMD formalism in SIDIS processes," *Journal of High Energy Physics*, vol. 2, article 95, 2015.

[20] J. Collins, L. Gamberg, A. Prokudin, T. Rogers, N. Sato, and B. Wang, "Relating transverse-momentum-dependent and collinear factorization theorems in a generalized formalism," *Physical Review D*, vol. 94, article 034014, 2016.

[21] J. Collins and T. C. Rogers, "Connecting different TMD factorization formalisms in QCD," *Physical Review D*, vol. 96, article 054011, 2017.

[22] M. G. Echevarria, T. Kasemets, J. Lansberg, C. Pisano, and A. Signori, "Matching factorization theorems with an inverse-error weighting," *Physics Letters B*, vol. 781, pp. 161–168, 2018.

[23] I. Scimemi and A. Vladimirov, "Analysis of vector boson production within TMD factorization," *The European Physical Journal C*, vol. 78, article 89, 2018.

[24] M. A. Ebert, I. Moult, I. W. Stewart et al., "Subleading power rapidity divergences and power corrections for q_T," 2018, https://arxiv.org/abs/1812.08189.

[25] I. Balitsky and A. Tarasov, "Power corrections to TMD factorization for Z-boson production," *Journal of High Energy Physics*, vol. 5, article 150, 2018.

[26] J. Collins, *Foundations of Perturbative QCD*, vol. 32 of *Cambridge Monographs on Particle Physics, Nuclear Physics and Cosmology*, Cambridge University Press, Cambridge, UK, 2011.

[27] G. Bozzi, S. Catani, G. Ferrera, D. de Florian, and M. Grazzini, "Production of Drell-Yan lepton pairs in hadron collisions: transverse-momentum resummation at next-to-next-to-leading logarithmic accuracy," *Physics Letters B*, vol. 696, pp. 207–213, 2011.

[28] S. Catani, D. de Florian, G. Ferrera, and M. Grazzini, "Vector boson production at hadron colliders: transverse-momentum resummation and leptonic decay," *Journal of High Energy Physics*, vol. 2015, no. 12, pp. 1–47, 2015.

[29] A. Bacchetta, M. G. Echevarria, P. J. Mulders, M. Radici, and A. Signori, "Effects of TMD evolution and partonic flavor on e^+ e^- annihilation into hadrons," *Journal of High Energy Physics*, vol. 11, article 76, 2015.

[30] D. Kang, C. Lee, and V. Vaidya, "A fast and accurate method for perturbative resummation of transverse momentum-dependent observables," *Journal of High Energy Physics*, vol. 4, article 149, 2018.

[31] S. Catani, L. Cieri, D. de Florian, G. Ferrera, and M. Grazzini, "Vector boson production at hadron colliders: hard-collinear coefficients at the NNLO," *The European Physical Journal C*, vol. 72, article 2195, 2012.

[32] M. G. Echevarria, I. Scimemi, and A. Vladimirov, "Unpolarized transverse momentum dependent parton distribution and fragmentation functions at next-to-next-to-leading order," *Journal of High Energy Physics*, vol. 9, article 4, 2016.

[33] G. Bozzi, S. Catani, D. de Florian, and M. Grazzini, "Transverse-momentum resummation and the spectrum of the Higgs boson at the LHC," *Nuclear Physics B*, vol. 737, no. 1-2, pp. 73–120, 2006.

[34] M. G. Echevarría, A. Idilbi, A. Schäfer, and I. Scimemi, "Model-independent evolution of transverse momentum dependent distribution functions (TMDs) at NNLL," *The European Physical Journal C*, vol. 73, article 2636, 2013.

[35] W. Bizoń, X. Chen, A. Gehrmann-De Ridder et al., "Fiducial distributions in Higgs and Drell-Yan production at $N^3LL+NNLO$," *Journal of High Energy Physics*, vol. 2018, article 132, 2018.

[36] S. M. Aybat and T. C. Rogers, "TMD parton distribution and fragmentation functions with QCD evolution," *Physical Review D*, vol. 83, article 114042, 2011.

[37] E. Laenen, G. Sterman, and W. Vogelsang, "Higher order QCD corrections in prompt photon production," *Physical Review Letters*, vol. 84, no. 19, pp. 4296–4299, 2000.

[38] D. Boer and W. J. den Dunnen, "TMD evolution and the Higgs transverse momentum distribution," *Nuclear Physics B*, vol. 886, pp. 421–435, 2014.

[39] D. Boer, "Linearly polarized gluon effects in unpolarized collisions," in *Proceedings of the QCD Evolution '15*, p. 23, October 2015.

[40] F. Landry, R. Brock, P. M. Nadolsky, and C. Yuan, "Tevatron Run-1 Z boson data and Collins-Soper-Sterman resummation formalism," *Physical Review D*, vol. 67, article 073016, 2003.

[41] R. D. Ball, V. Bertone, S. Carrazza et al., "Parton distributions for the LHC Run II," *Journal of High Energy Physics*, vol. 4, article 40, 2015.

[42] R. D. Ball, V. Bertone, S. Carrazza et al., "Parton distributions from high-precision collider data," *European Physical Journal C*, vol. 77, article 663, 2017.

[43] C. M. Carloni Calame, G. Montagna, O. Nicrosini, and M. Treccani, "Higher-order QED corrections to W-boson mass determination at hadron colliders," *Physical Review D*, vol. 69, article 037301, 2004.

[44] C. M. Carloni Calame, G. Montagna, O. Nicrosini, and M. Treccani, "Multiple photon corrections to the neutral-current Drell-Yan process," *Journal of High Energy Physics*, vol. 5, article 19, 2005.

[45] S. Quackenbush and Z. Sullivan, "Parton distributions and the W mass measurement," *Physical Review D*, vol. 92, article 033008, 2015.

[46] G. Bozzi, L. Citelli, M. Vesterinen, and A. Vicini, "Prospects for improving the LHC W boson mass measurement with forward muons," *The European Physical Journal C*, vol. 75, article 601, 2015.

[47] P. M. Nadolsky, H.-L. Lai, Q.-H. Cao et al., "Implications of CTEQ global analysis for collider observables," *Physical Review D*, vol. 78, article 013004, 2008.

[48] A. D. Martin, W. J. Stirling, R. S. Thorne, and G. Watt, "Parton distributions for the LHC," *The European Physical Journal C*, vol. 63, pp. 189–285, 2009.

[49] R. D. Ball, V. Bertone, F. Cerutti et al., "Impact of heavy quark masses on parton distributions and LHC phenomenology," *Nuclear Physics B*, vol. 849, no. 2, pp. 296–363, 2011.

[50] J. Gao, M. Guzzi, J. Huston et al., "CT10 next-to-next-to-leading order global analysis of QCD," *Physical Review D*, vol. 89, article 033009, 2014.

[51] L. A. Harland-Lang, A. D. Martin, P. Motylinski, and R. S. Thorne, "Parton distributions in the LHC era: MMHT 2014 PDFs," *The European Physical Journal C*, vol. 75, article 204, 2015.

[52] R. D. Ball, V. Bertone, S. Carrazza et al., "Parton distributions with LHC data," *Nuclear Physics B*, vol. 867, pp. 244–289, 2013.

[53] E. L. Berger and J. Qiu, "Differential cross section for Higgs boson production including all-orders soft gluon resummation," *Physical Review D*, vol. 67, article 034026, 2003.

[54] E. L. Berger and J. Qiu, "Differential cross-sections for Higgs boson production at Tevatron collider energies," *Physical Review Letters*, vol. 91, article 222003, 2003.

[55] E. L. Berger, J. Qiu, and Y. Wang, "Transverse momentum distribution of Υ production in hadronic collisions," *Physical Review D*, vol. 71, article 034007, 2005.

[56] E. C. Aschenauer, U. D'Alesio, and F. Murgia, "TMDs and SSAs in hadronic interactions," *The European Physical Journal A*, vol. 52, no. 6, 2016.

[57] C. Hadjidakis, D. Kikoła, J. P. Lansberg et al., "A fixed-target programme at the LHC: physics case and projected performances for heavy-ion, hadron, spin and astroparticle studies," 2018, https://arxiv.org/abs/1807.00603.

[58] D. Boer, M. Diehl, R. Milner et al., "Gluons and the quark sea at high energies: distributions, polarization, tomography," 547 pages, 2011, https://arxiv.org/abs/1108.1713.

[59] J. Dudek, R. Ent, R. Essig et al., "Physics opportunities with the 12 GeV upgrade at jefferson lab," *European Physical Journal A*, vol. 48, article 187, 2012.

[60] A. Accardi, J. L. Albacete, M. Anselmino et al., "Electron ion collider: the next QCD frontier," *The European Physical Journal A*, vol. 52, article 268, 2016.

[61] R. Angeles-Martinez, A. Bacchetta, I. Balitsky et al., "Transverse momentum dependent (TMD) parton distribution functions: status and prospects," *Acta Physica Polonica B*, vol. 46, no. 12, pp. 2501–2534, 2015.

[62] M. Diehl, "Introduction to GPDs and TMDs," *The European Physical Journal A*, vol. 52, article 149, 2016.

[63] M. Boglione and A. Prokudin, "Phenomenology of transverse spin: past, present and future," *The European Physical Journal A*, vol. 52, article 154, 2016.

[64] A. Bacchetta, "Where do we stand with a 3-D picture of the proton?" *The European Physical Journal A*, vol. 52, article 163, 2016.

[65] D. Boer, S. Cotogno, T. van Daal et al., "Gluon and Wilson loop TMDs for hadrons of spin ≤ 1," *Journal of High Energy Physics*, vol. 10, article 13, 2016.

[66] A. Metz and A. Vossen, "Parton fragmentation functions," *Progress in Particle and Nuclear Physics*, vol. 91, pp. 136–202, 2016.